nature publishing group

Heparin-binding EGF-like growth factor promotes neuronal nitric oxide synthase expression and protects the enteric nervous system after necrotizing enterocolitis

Yu Zhou[1], Yijie Wang[1], Jacob Olson[1], Jixin Yang[1] and Gail E. Besner[1]

BACKGROUND: Neonatal necrotizing enterocolitis (NEC) is associated with alterations of the enteric nervous system (ENS), with loss of neuronal nitric oxide synthase (nNOS)-expressing neurons in the intestine. The aim of this study was to investigate the roles of heparin-binding EGF-like growth factor (HB-EGF) in neural stem cell (NSC) differentiation, nNOS expression, and effects on ENS integrity during experimental NEC.

METHODS: The effects of HB-EGF on NSC differentiation and nNOS production were determined using cultured enteric NSCs. Myenteric neuronal subpopulations were examined in HB-EGF knockout mice. Rat pups were exposed to experimental NEC, and the effects of HB-EGF treatment on nNOS production and intestinal neuronal apoptosis were determined.

RESULTS: HB-EGF promotes NSC differentiation, with increased nNOS production in differentiated neurons and glial cells. Moreover, loss of nNOS-expressing neurons in the myenteric plexus and impaired neurite outgrowth were associated with absence of the HB-EGF gene. In addition, administration of HB-EGF preserves nNOS expression in the myenteric plexus and reduces enteric neuronal apoptosis during experimental NEC.

CONCLUSION: HB-EGF promotes the differentiation of enteric NSCs into neurons in a nitric oxide (NO)-dependent manner, and protects the ENS from NEC-induced injury, providing new insights into potential therapeutic strategies for the treatment of NEC in the future.

Necrotizing enterocolitis (NEC) is the most common type of gastrointestinal emergency in neonates. The enteric nervous system (ENS) is an autonomous collection of neurons and supportive cells in the gut wall, and an immature ENS has been observed in premature infants, characterized by decreased organized intestinal motility (1). The intrinsic ENS immaturity or the subsequent intestinal dysmotility may make preterm babies more vulnerable to developing NEC. Intestinal motility is mainly regulated by neurotransmitters produced by myenteric neurons. Neuronal nitric oxide synthase (nNOS)-producing neurons and choline acetyl transferase (ChAT)-producing neurons are two major intestinal neuronal subpopulations involved in the regulation of intestinal motility, and nNOS/ChAT misbalance has been reported in certain inflammatory intestinal diseases and genetic intestinal motility disorders (2,3). We have shown that neonatal NEC is associated with alterations of the ENS, with significant loss of nNOS-expressing neurons not only in the acute stages of the disease but also months later at the time of stoma closure (4). This decreased nNOS expression may explain the intestinal dysmotility seen in NEC patients even after recovery from the acute event. Current therapy for intestinal dysmotility is limited mainly to palliation, and new treatments for this debilitating condition are clearly needed.

Heparin-binding EGF-like growth factor (HB-EGF) is a member of the epidermal growth factor superfamily (5), and we have shown that administration of enteral HB-EGF, or overexpression of HB-EGF in transgenic mice, increases resistance to NEC (6), whereas HB-EGF knockout (KO) mice have increased susceptibility to NEC (7). We have also shown that HB-EGF is widely expressed in enteric ganglia, improves enteric neural progenitor survival and migration, encourages neurite outgrowth, and promotes ENS development (8–10). In addition, we demonstrated that HB-EGF is present in human amniotic fluid and breast milk, ensuring continuous exposure of the fetal and newborn intestine to the growth factor (11). HB-EGF may serve an important role in augmenting ENS development and intestinal neuronal functions in the fetal and early infantile stage. In this study, we aimed to assess the effects of HB-EGF on NSC differentiation and functional expression of nNOS, and test the effects of HB-EGF on the ENS and on the specific cell fate of enteric neural progenitors during NEC injury.

METHODS

Animals

All animal procedures were approved by the Institutional Animal Care and Use Committee of the Research Institute at Nationwide Children's Hospital (Protocol #04203AR and 06-00092AR). Time pregnant

[1]Department of Pediatric Surgery, The Ohio State University College of Medicine, Center for Perinatal Research, The Research Institute at Nationwide Children's Hospital, Columbus, Ohio. Correspondence: Yu Zhou (yu.zhou@nationwidechildrens.org)

Received 5 July 2016; accepted 8 February 2017; advance online publication 24 May 2017. doi:10.1038/pr.2017.68

Sprague–Dawley rats were purchased from Harlan Sprague–Dawley (Indianapolis, IN). HB-EGF KO mice on a C57BL/6J × 129 background and their HB-EGF WT C57BL/6J × 129 counterparts were kindly provided by David Lee (Chapel Hill, NC).

Primary Neurosphere Culture of NSCs

Enteric NSC isolation was performed as per our previously published methods (4). Intestinal LMMP was stripped from 2- to 3-day-old rat pups and subjected to enzymatic digestion and mechanic dissociation. Cells were cultured in NSC culture medium consisting of DMEM/F12 with 100 U/ml penicillin and 100 µg/ml streptomycin (Invitrogen, Carlsbad, CA), supplemented with 2 mmol/l L-glutamine 7.5% (v/v) chick embryo extract (Gemini Bio-products, West Sacramento, CA), N_2 medium supplement, 20 ng/ml mouse basic fibroblast growth factor, and 20 ng/ml mouse epidermal growth factor (Sigma-Aldrich, St Louis, MO). NSCs grew as free-floating cellular aggregates known as neurosphere-like bodies, which were mechanically dissociated every 7–10 days.

In vitro NSC Differentiation Assay

Dissociated neurospheres were seeded in poly-D-Lysine/Laminin-coated eight-well chamber slides (BD Biosciences, Bedford, MA) at a density of 5,000 cells per well. Subsequently, NSCs were cultured as monolayers in a differentiation medium containing NeuroBasal basal medium supplemented with B27 (Gibco, Grand Island, NY, USA), 2 mmol/l L-glutamine, and 1% fetal bovine serum, but lacking growth factors. A subset of NSCs were treated with 50 ng/ml HB-EGF for 3 days. One dose of the non-selective NOS inhibitor L-NAME (1 mM) or SIs of NOS was added to the cultured cells alone or for 30 min prior to the addition of HB-EGF. The NOS SI used included the nNOS SI ARL17477 (1 µM), the eNOS SI L-NIO dihydrochloride (10 µM), and the iNOS SI (S)-Methylisothiourea sulfate (100 µM; Tocris Bioscience, Pittsburgh, PA). After treatment for 3 days, cells were subjected to ICC, morphology analysis, or western blotting.

Primary Cultures of Myenteric Neurons and Neurite Outgrowth Measurement

E12.5 mouse embryonic guts were dissected from time pregnant HB-EGF KO or WT mice. After enzymatic digestion and mechanic dissociation, cell suspensions were incubated with p75NTR antibody (1:1,000, EMD Millipore, Billerica, MA) and goat anti-rabbit-coupled paramagnetic beads (Miltenyi Biotec, San Diego, CA, USA). After separation of p75NTR-expressing cells using a MACS Separation column (Miltenyi Biotec), immunoselected cells were plated at 5,000 cells/well on poly-D-Lysine/Laminin-coated chamber slides. Cells were cultured in NeuroBasal media containing 4% chicken embryo extract, 1% B27, 2 mmol/l glutamine, and 2% fetal bovine serum for 48 h before fixation with 4% paraformaldehyde (PFA), and were analyzed by ICC using anti-PGP9.5 antibody (Invitrogen). Cell processes extending from cell bodies were individually traced using ImagePro plus software (Media Cybernetics, Silver Springs, MD) and neurites were defined as processes longer than 10 µm in length. Cells bearing neurites were counted and the length of neurite outgrowth was measured. Quantification was performed on more than 100 intestinal neuronal cells isolated from each WT and KO animal ($n = 3$ animals from each group), and the percentage of neurite-bearing cells as well as the total neurite length per neuron was calculated.

ICC and IHC

Cultured cells or paraffin-embedded intestinal cross-sections were subjected to ICC or IHC. Cells or tissues were stained with the following antibodies: anti-Rat-401 (Nestin, 1:100, DSHBUI, Iowa City, IA), anti-Tuj-1 (1 µg/ml; clone 5G8; Promega, Madison, WI), anti-HuC/D (10 µg/ml, Invitrogen), anti-GFAP (1:1,000; Millipore, Billerica, MA), anti-nNOS (2 µg/ml), anti-ChAT (1:10, Millipore), followed by species-specific secondary antibodies conjugated to Cy2 or Cy3, respectively (Invitrogen or Jackson ImmunoResearch Laboratories, West Grove, PA). For whole-mount IHC of LMMP, intestinal tissue strips were dissected from the anti-mesenteric border of the intestines, and the LMMP layers were incubated with primary antibodies for 2 days. Fluorescence images were captured with confocal microscopy (LSM 710, Carl Zeiss, Thornwood, NY). nNOS-positive neurons were identified as immunoreactive for both nNOS and HuC/D, and ChAT-positive neurons were immunoreactive for both ChAT and HuC/D. nNOS-positive neurons and ChAT-positive neurons were counted, and the percentage of nNOS-positive or ChAT-positive neurons/total HuC/D stained neurons in WT or KO MPs was calculated.

Flow Cytometry

Briefly, NSCs or differentiating cells were fixed and permeabilized using an intracellular staining/permeabilization kit (Biolegend, San Diego, CA) according to the manufacturer's recommendation. After blocking, cells were incubated with primary antibodies such as mouse anti-Tuj-1 antibody (clone 5G8; Promega), rabbit anti-nNOS/NOS I antibody (Millipore), or mouse anti-GFAP antibody (Millipore). The cells were then stained with fluorescent-conjugated secondary anti-mouse phycoerythrin (PE) (Cell Signaling Technology, Danvers, MA, USA) or anti-rabbit APC (Santa Cruz Biotechnology, Santa Cruz, CA) in the dark for 30 min. Cells were evaluated with the BD LSR II flow cytometer (BD Biosciences). Data were analyzed using FlowJo software (version 7.6.5, Ashland, OR). To identify cell subpopulations, data are presented as the percentage of positive cells per total number of cells. To quantify surface antigen (Ag) expression, data are presented as the relative fold increase of the geometric mean over antibody control (mean ± s.e.m.).

Real-Time Reverse-Transcription-PCR

Total RNA isolated from cell lysates was reverse-transcribed with random hexamers using a first-strand cDNA synthesis kit (Invitrogen). Real-time RT-PCR was carried out using an SYBR Green RT-PCR kit (Applied Biosystems, Branchburge, NJ) and an ABI Prism 770 Sequence Detection System (Applied Biosystems). Nestin and Sox2 were amplified using the following primers: Nestin sense: 5′-GTCTCAGGACAGTGCTGAGCCTTC-3′, Nestin antisense: 5′-TCCCCTGAGGACCAGGAGTCTC-3′; Sox2 sense: 5′-CCTCCG GGACATGATCAGCATGTA-3′, Sox2 antisense: 5′-GCAGTGTG CCGTTAATGGCCGTG-3′. Amplification of the housekeeping gene (GAPDH) cDNA was used as an internal control for quantification. Quantification was performed using Relative Quantification Software, version 1.01 (Applied Biosystems).

Western Blotting

Cells or LMMP strips of intestine from rat pups were harvested and cell or tissue lysates were subjected to SDS-PAGE and immunoblot analysis. Peripherin, GFAP, nNOS, ChAT, and proliferating cell nuclear antigen (EMD Millipore) were detected using primary antibodies followed by horseradish peroxidase-conjugated secondary antibodies. The intensity of immunoreative bands on western blotting images was quantified using the Scion Image Program (Scion Corporation, Frederick, MD) and was expressed as mean ± s.e.m. For western blotting of myenteric neuronal subpopulations, LMMP strips were dissected from 4- to 6-week-old HB-EGF WT and KO mice.

Animal Model of Experimental NEC

Experimental NEC was induced as we have previously described (12). Timed pregnant Sprague–Dawley rats underwent Cesarean section on day 21 of gestation (E21). Newborn rat pups in the experimental NEC group were gavage-fed with hypertonic formula containing 15 g Similac 60/40 (Ross Pediatrics, Columbus, OH) in 75 ml Esbilac (Pet-Ag, New Hampshire, IL), a diet that provided 836.8 kJ/kg daily. Pups were exposed to hypoxia with 100% nitrogen for 1 min followed by hypothermia at 4 °C for 10 min twice daily beginning 60 min after birth for 4 days, with intragastric administration of lipopolysaccharide (2 mg/kg, Sigma-Aldrich) 8 h after birth. Pups treated with enteral HB-EGF received 800 µg/kg/dose

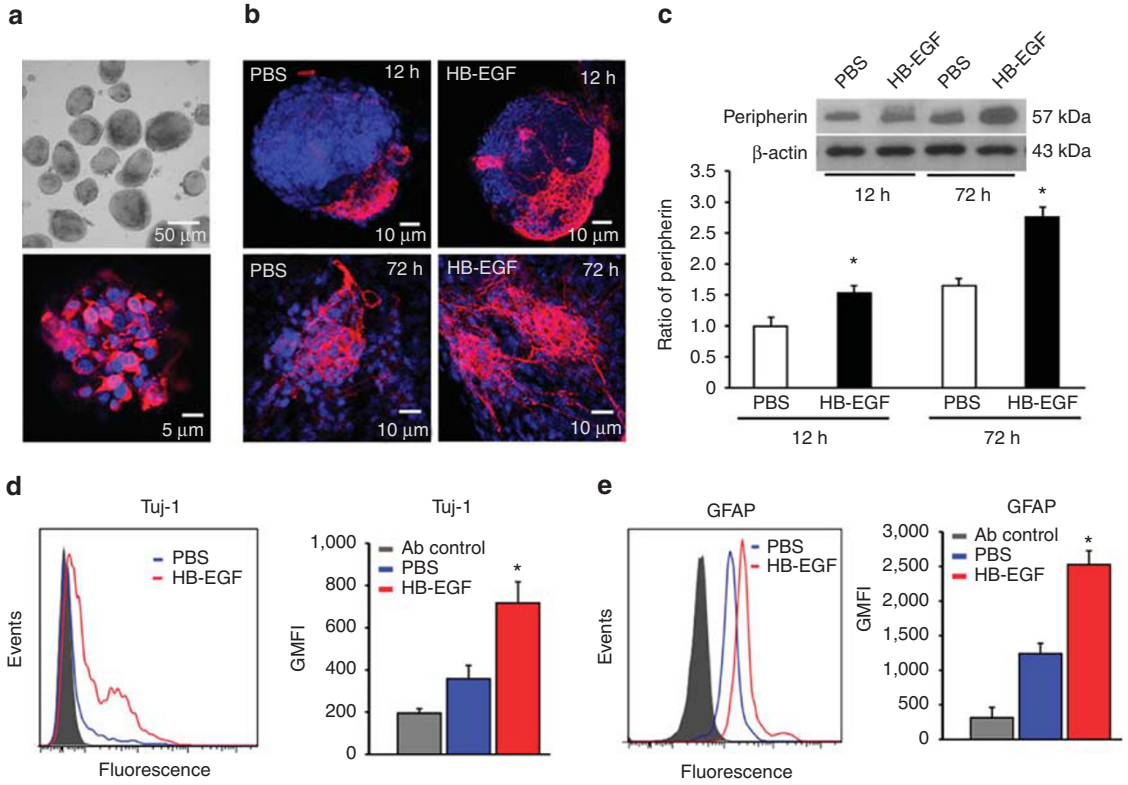

Figure 1. HB-EGF promotes NSC differentiation. NSCs were derived from LMMP strips and cultured. (**a**) Phase-contrast image of NSC expanded in culture to form neurosphere-like bodies (upper panel) and fluorescence immunocytochemistry image of undifferentiated neurospheres stained for the NSC marker nestin (lower panel). (**b**) Dissociated neurospheres were seeded onto poly-D-lysine-Laminin-coated chamber slides and incubated in differentiation medium to induce differentiation in the presence or absence of HB-EGF (50 ng/ml) for 12 and 72 h; the cells were then immunostained with Tuj-1 antibody (red) to identify differentiated neurons. There was a marked increase in the number of Tuj-1-positive cells in the peripheral areas of the neurospheres after 12 h in the presence of HB-EGF, and increased Tuj-1-positive cells with neurite extensions were noted after 72 h of HB-EGF treatment. (**c**) Cell lysates were subjected to immunoblot analysis using antibodies to the neuronal cell marker peripherin. Densitometry results were normalized to β-actin and expressed as mean ± s.e.m. $n = 3$ independent experiments. Compared with control cells, HB-EGF-treated cells had significantly increased peripherin protein levels after incubation with HB-EGF for 12 and 72 h. *$P < 0.05$ for HB-EGF vs. PBS. (**d**,**e**) Representative flow cytometry histograms for the expression of Tuj-1 (neuron marker) and GFAP (glial cell marker) in differentiating neurospheres treated with HB-EGF (red line) or PBS (blue line). GMFI showing differences for Tuj-1 and GFAP as mean ± s.e.m. ($n = 3$ independent experiments). GMFI, geometric mean fluorescence intensity. GFAP, glial fibrillary acid protein; HB-EGF, heparin-binding EGF-like growth factor; LMMP, longitudinal muscle myenteric plexus; NSC, neural stem cell; PBS, phosphate-buffered saline. *$P < 0.05$ for HB-EGF vs. PBS (Student's *t*-test).

added to each feed. Pups were killed by cervical dislocation upon the development of any clinical signs of NEC, or at the end of the experiment at 4 days after birth. Normal control pups, designated as the breast milk group, were breast-fed using surrogate mothers and were not exposed to stress.

Neuronal Apoptosis and ENS Degeneration Evaluation

Cross-sections (4 µm thickness) from rat pup intestinal specimens were used to identify enteric ganglia in submucosal plexuses and MP located between the mucosal and intramuscular layers. Ten serial sections from individual animals were examined in order to reduce the possibility of biased observations. Sections were subjected to IHC using anti-HuC/D to recognize intestinal neurons, and were then subjected to a TUNEL assay using the ApopTag Fluorescein *in situ* Apoptosis Detection Kit (EMD Millipore). Apoptotic neurons were defined as those that stained positive for both TUNEL and HuC/D. Apoptotic neurons in submusocal ganglia and myenteric ganglia were counted, and the percentage of apoptotic neurons/total HuC/D immunoreactive neurons was calculated. To further identify ENS degeneration, FluoroJade C histochemical staining was performed. After incubation in 0.06% w/v $KMnO_4$ solution for 2 min, sections were stained with 0.0004% w/v FluoroJade C (Histo-Chem, Jefferson, AR) in 0.1% v/v acetic acid solution for 30 min. The same sections were subjected to IHC using anti-HuC/D antibody to recognize intestinal neurons. Degenerative neurons in the ENS were identified with FluoroJade C-positive staining cells. Degenerative neurons in the submusocal ganglia and myenteric ganglia were counted, and the percentage of degenerative neurons/HuC/D immunoreactive neurons was calculated.

Statistical Analyses

All data are presented as mean ± s.e.m. Statistical analyses were performed using the Student *t*-test or one-way analysis of variance, and Dunnett's *post hoc* analysis if needed (SigmaPlot 11.0, Systat Software, San Jose, CA). *P* values < 0.05 were considered statistically significant.

RESULTS

HB-EGF Increases Neural and Glial Cell Protein Expression During Neurosphere Differentiation

NSCs from longitudinal muscle myenteric plexus (LMMP) strips were cultured in selective growth medium to allow them

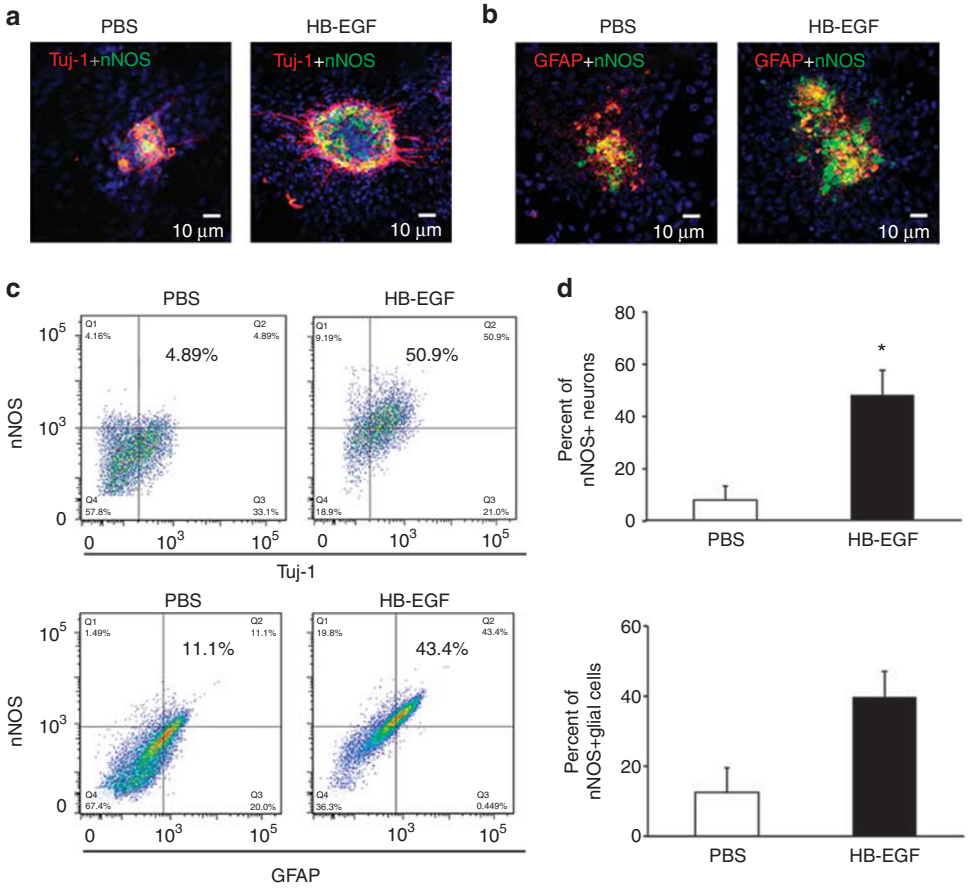

Figure 2. HB-EGF enhances nNOS production in differentiated neurons and glial cells. (**a**,**b**) Representative ICC images of differentiating neurospheres double-stained with candidate cell markers (red) and nNOS (green) demonstrating nNOS expression in neurons (**a**) and glial cells (**b**). Incubation with HB-EGF for 3 days led to increased numbers of differentiated neurons expressing nNOS ($Tuj1^+nNOS^+$) and differentiated glial cells expressing nNOS ($GFAP^+nNOS^+$). Scale bar = 10 µm. (**c**) Representative FACS plots of differentiating neurospheres co-labeled with candidate cell markers and nNOS antibodies, showing differentiated neurons labeled with Tuj-1 and nNOS antibodies, and differentiated glial cells labeled with GFAP and nNOS antibodies. Quadrant boundaries were determined by thresholds for non-specific labeling using the control antibody IgG_2 and gating was performed on $nNOS^+Tuj\text{-}1^+$ or $nNOS^+GFAP^+$ cells. The top right quadrants identify $Tuj\text{-}1^+nNOS^+$ cells and $GFAP^+nNOS^+$ cells, respectively. (**d**) Quantification of data from **c**. Data represent the mean ± s.e.m. of five independent experiments. Addition of HB-EGF significantly increases $Tuj\text{-}1^+nNOS^+$ cells and $GFAP^+nNOS^+$ cells. $^*P < 0.05$ for HB-EGF vs. PBS (Student' *t*-test). FACS, fluorescence-activated cell sorting; GFAP, glial fibrillary acid protein; HB-EGF, heparin-binding EGF-like growth factor; ICC, immunocytochemistry; nNOS, neuronal nitric oxide synthase; PBS, phosphate-buffered saline.

to expand to form neurosphere-like bodies (**Figure 1a**). Undifferentiated neurospheres expressed high levels of the NSC marker nestin (**Figure 1a**). Following differentiation in induction medium, enteric NSCs are known to differentiate into neurons and glial cells, which express high levels of the neuronal-specific marker Tuj-1 and the glial marker glial fibrillary acid protein (GFAP), respectively (4). To investigate the effects of HB-EGF on NSC differentiation, NSCs were cultured in the presence of HB-EGF (50 ng/ml) for 12 and 72 h and then immunostained with Tuj-1 antibody. There was a marked increase in the number of Tuj-1-positive cells with neurite extensions after HB-EGF treatment (**Figure 1b**). Neurosphere-derived cells had significantly increased protein levels of the neuronal differentiation marker peripherin after incubation with HB-EGF for 12 or 72 h (**Figure 1c**). Flow cytometry confirmed significantly increased levels of Tuj-1 and GFAP protein in HB-EGF-treated cells compared with control cells (**Figure 1d,e**). These findings demonstrate that HB-EGF promotes NSC differentiation into neurons and glial cells.

HB-EGF Enhances nNOS Production During Differentiation of NSCs

Previous reports have shown that nitric oxide (NO) is involved in neural differentiation and synaptic plasticity (13). To understand the roles of HB-EGF in NO production during differentiation, we next investigated whether HB-EGF promotes expression of neuronal NOS, a major NOS isoform, to produce NO. After 3 days of HB-EGF exposure, neurosphere-derived cells showed a significant increase in the number of nNOS-immunoreactive cells ($nNOS^+$), which were also immunoreactive to either Tuj-1 ($Tuj\text{-}1^+$) or GFAP ($GFAP^+$; **Figure 2a,b**). Flow cytometry confirmed a significant increase in the proportion of nNOS-positive

neurons (nNOS$^+$Tuj-1$^+$; 47.9 ± 9.6% vs. 7.8 ± 5.24%) and nNOS-positive glial cells (nNOS$^+$GFAP$^+$; 39.6 ± 7.5% vs. 12.7 ± 6.9%) in HB-EGF-treated cells compared with control cells (Figure 2c,d). These findings further demonstrate that HB-EGF promotes NSC differentiation into nNOS-positive neurons or nNOS-positive glial cells.

Inhibition of Endogenous NO Production Inhibits the Ability of HB-EGF to Promote Neuronal Differentiation

To further investigate whether HB-EGF-induced neural differentiation is NO-dependent, the non-selective NOS inhibitor L-NAME (L-N, G-Nitroarginine methyl ester; 1 mM) was added to the culture medium of NSC either alone

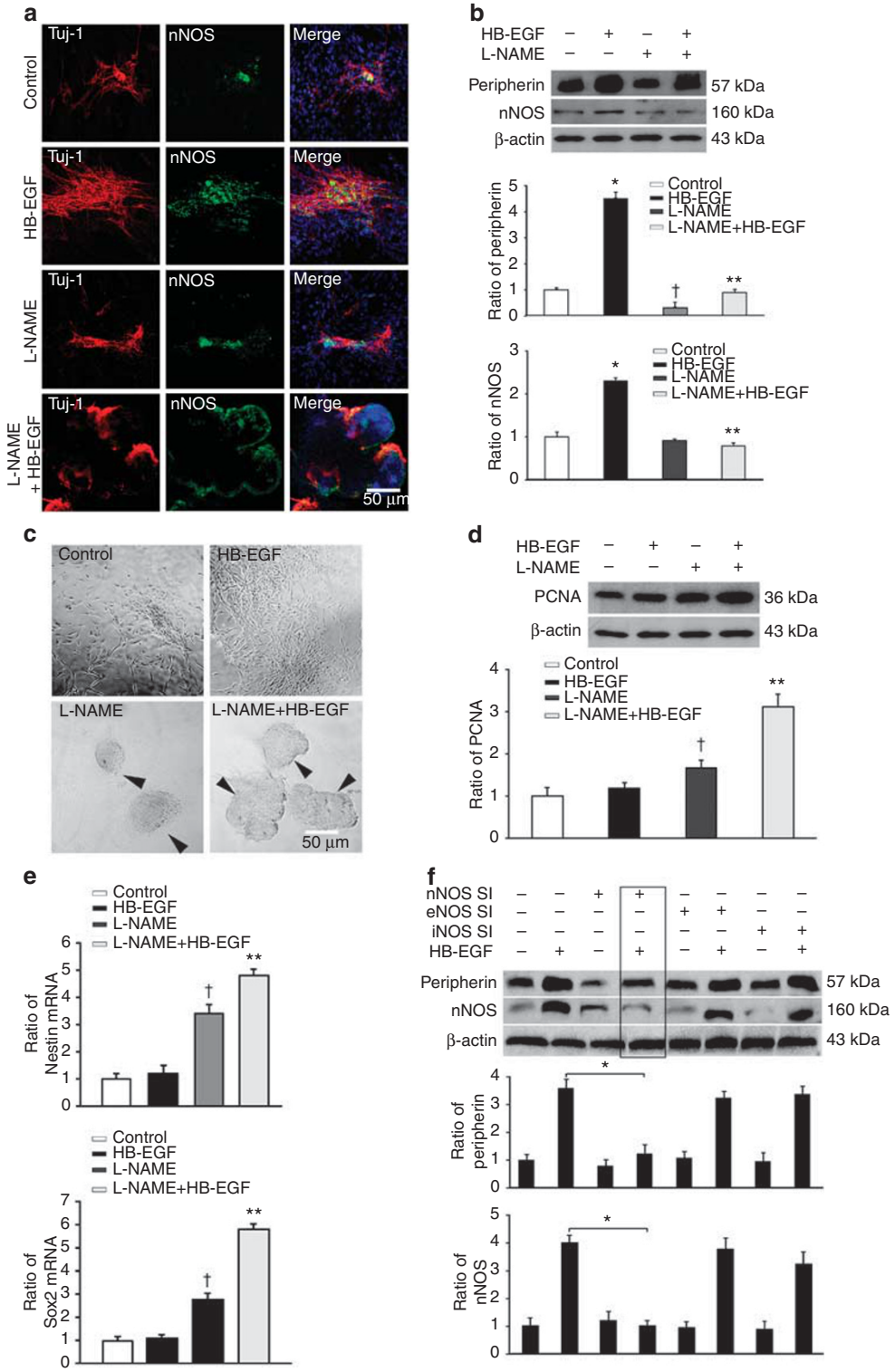

or 30 min prior to the addition of HB-EGF. After 3 days of treatment, immunocytochemistry (ICC) showed that the protein levels of nNOS and the neuronal marker Tuj-1 were significantly decreased in cells treated with L-NAME (**Figure 3a**). Western blot detection of nNOS and the neuronal marker peripherin showed similar findings (**Figure 3b**), confirming that HB-EGF-induced neural differentiation is NO-dependent. Interestingly, cells switched from a neural fiber-like phenotype to an appearance resembling proliferating neurospheres after 3 days of exposure to L-NAME+HB-EGF (**Figure 3c**), indicating that NOS inhibition blocks the ability of HB-EGF to promote neural differentiation. Western blotting showed that proliferating cell nuclear antigen protein levels were significantly increased after treatment with either L-NAME alone or L-NAME+HB-EGF, suggesting that NOS inhibition may switch NSC from a state of differentiation to a state of proliferation (**Figure 3d**). Real-time reverse-transcriptase-PCR analysis of the treated cells showed that mRNA expression levels of the NSC proliferation markers Nestin and Sox2 were significantly increased after L-NAME+HB-EGF treatment (**Figure 3e**). To confirm that the effects of HB-EGF on NSC differentiation are nNOS-dependent, selective inhibitors (SIs) of NOS isoforms were applied. nNOS-SI ARL17477 significantly reduced HB-EGF-induced peripherin production (**Figure 3f**), indicating that nNOS, but not the other NOS isoforms, is a critical factor in HB-EGF-induced neural differentiation.

Deletion of the HB-EGF Gene is Associated with a Decrease in nNOS-Positive Neurons in the Intestine

As we have previously reported that HB-EGF is expressed in the ENS (9), and as HB-EGF promotes nNOS expression during NSC differentiation, we next investigated whether loss of HB-EGF leads to ENS alteration. We dissected LMMP from the ileum of wild-type (WT) and HB-EGF KO mice and performed whole-mount immunohistochemistry (IHC) of myenteric ganglia to identify ganglionated plexus neurons and characterize two major myenteric neuronal subtypes: nNOS and ChAT. We demonstrated significant abnormalities in the myenteric plexuses (MPs) of HB-EGF KO mice, including significantly decreased numbers of nNOS-positive neurons (**Figure 4a,b**), and significantly increased numbers of ChAT-positive neurons in the MP (**Figure 4c,d**). Western blotting confirmed significantly decreased levels of nNOS and significantly increased levels of ChAT in the LMMP of HB-EGF KO mice (**Figure 4e,f**). Primary cultures of intestinal neurons from embryonic guts of HB-EGF KO mice showed significantly shorter neurite length and significantly decreased numbers of neurons extending neurites compared with WT mice (**Figure 4g,h**). These findings confirmed that HB-EGF is involved in the regulation of intestinal functional neuronal subtypes during ENS development, with absence of HB-EGF associated with impaired neurite outgrowth.

HB-EGF Preserves nNOS Expression in the MP and Protects Neurons from NEC-Induced Injury

We recently reported that clinical NEC is associated with alterations of the ENS, with significant loss of nNOS-positive neurons. We next examined the effects of administration of HB-EGF on the ENS during experimental NEC. We found compromised ENS integrity including loss of neurons and glial cells and reduced nNOS-positive cells in the intestine of rat pups exposed to NEC. However, in pups that were exposed to NEC that received HB-EGF added to the feeds, ENS integrity was maintained and nNOS expression was preserved (**Figure 5**). The ability of HB-EGF to restore ENS integrity was further confirmed by neuronal apoptosis examination. Terminal deoxynucleotidyl transferase nick-end labeling (TUNEL) analysis of intestinal sections revealed dense TUNEL staining in HuC/D-immunoreactive neurons upon exposure to NEC, whereas treatment with HB-EGF markedly reduced neuronal apoptosis in the intestine of rat pups

Figure 3. The effect of HB-EGF on neuronal differentiation is nNOS- and NO-dependent. (**a**) NSCs were grown in differentiation medium with the addition of HB-EGF (50 ng/ml) alone, the non-selective NOS inhibitor L-N, G-Nitroarginine methyl ester (L-NAME) alone (1 mM), or with L-NAME for 30 min followed by HB-EGF. PBS was used as control. After 3 days of treatment, cells were fixed and immunostained with antibodies to either Tuj-1 (red) or nNOS (green). 4,6-Diamidino-2-phenylindole (DAPI) was used to counterstain nuclei. Scale bar = 50 μm. (**b**) Cell lysates were subjected to immunoblot analysis using antibodies to the neuronal cell marker peripherin and nNOS. Densitometry results were normalized to β-actin and expressed as mean ± s.e.m. $n = 3$ independent experiments. There were significantly increased protein levels of nNOS and peripherin in HB-EGF-treated cells compared with control cells, which was blocked by addition of L-NAME. $^{*}P < 0.05$ for HB-EGF vs. PBS control; $^{\dagger}P < 0.05$ for L-NAME vs. control; $^{**}P < 0.05$ for L-NAME+HB-EGF vs. HB-EGF. (**c**) Morphology of NSC exposed to HB-EGF alone, L-NAME alone, or L-NAME followed by HB-EGF. Noted the increased number of neurons with neurite extensions in the presence of HB-EGF, and the increased numbers of round, compact spheroids in the presence of L-NAME or L-NAME+HB-EGF (arrowheads). Scale bar = 50 μm. (**d**) Immunoblot analysis using antibodies to PCNA. Densitometry results were normalized to β-actin and expressed as mean ± s.e.m. $n = 3$ independent experiments. Compared with control NSC, NSC with the addition of L-NAME alone or L-NAME+HB-EGF had significantly increased PCNA protein levels. $^{\dagger}P < 0.05$ for L-NAME vs. control; $^{**}P < 0.05$ for L-NAME +HB-EGF vs. L-NAME. (**e**) mRNA expression of Nestin and Sox2 as determined by real-time reverse-transcriptionPCR. $^{\dagger}P < 0.05$ for L-NAME vs. control; $^{**}P < 0.05$ for L-NAME+HB-EGF vs. L-NAME. (**f**) NSCs were grown in differentiation medium in the presence of a NOS SI alone or a SI for 30 min followed by HB-EGF (50 ng/ml). The NOS SIs used included nNOS SI ARL17477 (1 μM), eNOS SI L-NIO dihydrochloride (10 μM), and iNOS SI S-Methylisothiourea sulfate (100 μM). After incubation for 3 days, cell lysates were subjected to western blotting using anti-peripherin and anti-nNOS antibodies. Densitometry results were normalized to β-actin. HB-EGF induced an increase in peripherin and nNOS protein levels that was blocked by the nNOS SI only. $^{*}P < 0.05$ for nNOS SI+HB-EGF vs. HB-EGF (ANOVA with Dunnett's *post hoc* analysis). $n = 3$ independent experiments. ANOVA, analysis of variance; FACS, fluorescence-activated cell sorting; HB-EGF, heparin-binding EGF-like growth factor; nNOS, neuronal nitric oxide synthase; NO, nitric oxide; PBS, phosphate-buffered saline; PCNA, proliferating cell nuclear antigen; SI, selective inhibitor.

subjected to NEC (Figure 6a). Quantification of TUNEL-stained neurons in the submucosal and MPs demonstrated that HB-EGF significantly decreased apoptotic neurons in the ENS after NEC injury (Figure 6b). In addition, pups exposed to NEC that were treated with HB-EGF had significantly decreased numbers of degenerated neurons, as recognized with FluorJade C dye staining (Figure 6c,d).

DISCUSSION

Emerging evidence has shown that during embryonic and postnatal stages, HB-EGF demonstrates a specific temporal and spatial pattern in the ENS and the brain, supporting its function in the development and remodeling of the nervous systems (9,14). In the present study, we demonstrated that HB-EGF promotes enteric NSC differentiation and enhances

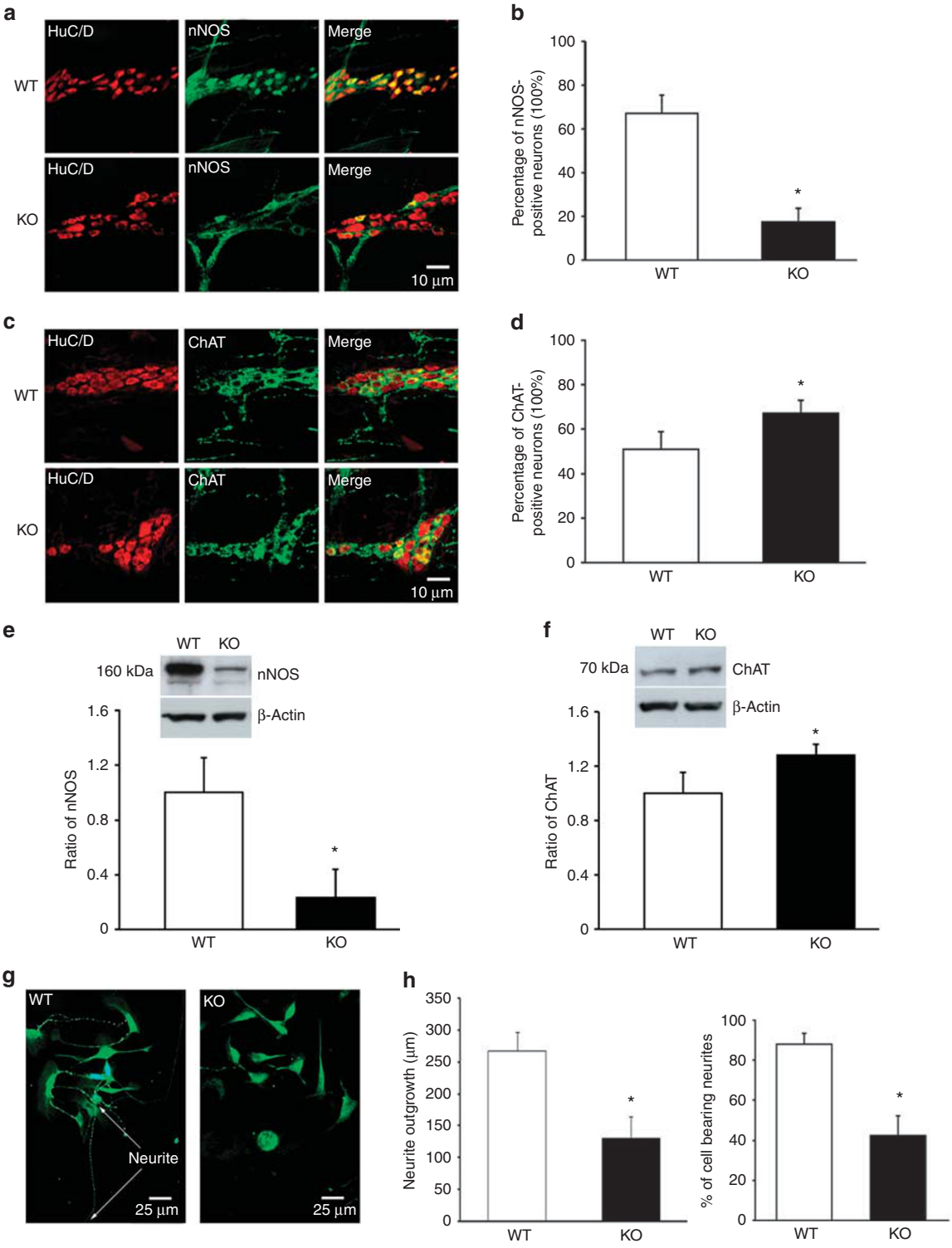

the expression of nNOS in differentiated neurons and glial cells. We also found that NO mediates the ability of HB-EGF to regulate enteric NSC differentiation. NO has been implicated in many different aspects of neuronal function, including neurite outgrowth, synaptic transmission, plasticity, and neuromodulation (15). As a major isoform in the ENS for NO production, nNOS is constitutively expressed to synthesize NO in a regulated manner. In mice, nNOS-containing neurons are the early neuronal subtypes associated with the NSC migratory wave front in fetal gut, with NOS immunoreactivity identified in the proximal midgut in early embryonic stages (16). NO release from newly formed nNOS-expressing neurons has been implicated as an inducing signal that promotes NSC migration into the intestine, with early

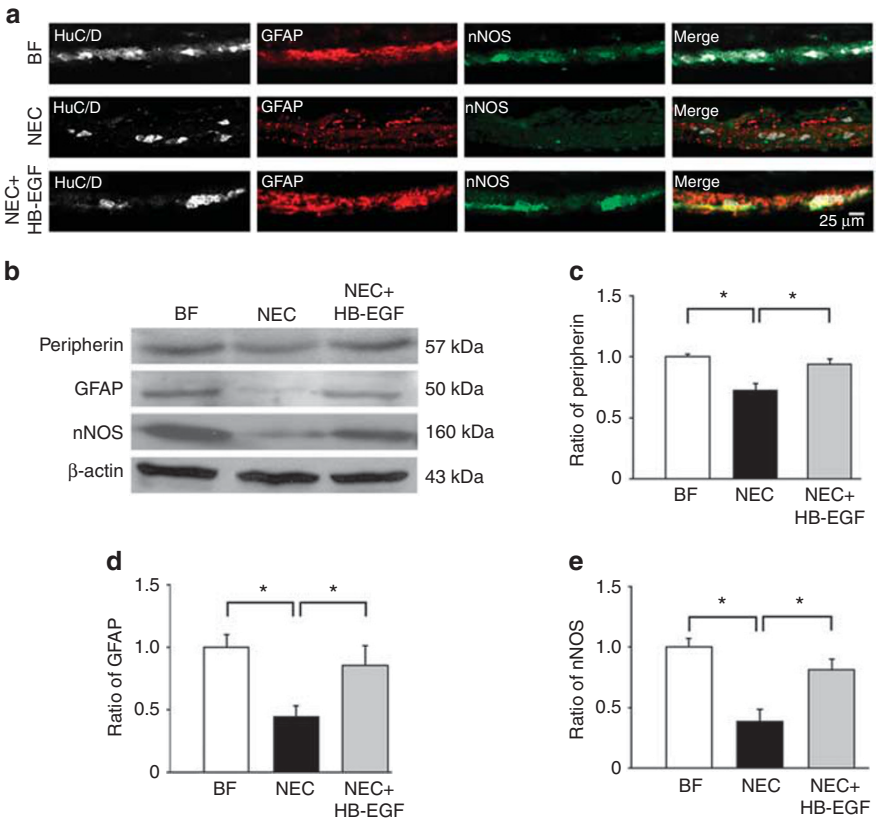

Figure 5. HB-EGF preserves intestinal neuronal and glial integrity and nNOS expression after NEC-induced injury. Pups were exposed to BF only, NEC, or NEC+HB-EGF. (**a**) Representative immunostaining images of ileal tissue sections using antibodies to HuC/D, GFAP, and nNOS to identify neurons, glial cells, and nNOS-producing cells, respectively. Scale bar = 25 µm. (**b**) Representative image of western blotting for the expression markers of neurons, glial cells, and nNOS-positive cells. Protein lysates of the intestinal intramuscular layers from three rat pups were loaded onto SDS-PAGE gels and probed with anti-peripherin, anti-GFAP, or anti-nNOS antibodies. (**c**–**e**) Densitometry results for Peripherin, GFAP, and nNOS normalized to β-actin and expressed as mean ± s.e.m. $^*P < 0.05$ (Dunnett's *post hoc* analysis). $n = 3$ independent experiments. BF, breast feeding; GFAP, glial fibrillary acid protein; HB-EGF, heparin-binding EGF-like growth factor; NEC, neonatal necrotizing enterocolitis; nNOS, neuronal nitric oxide synthase.

Figure 4. nNOS is decreased in the myenteric plexuses of HB-EGF KO mice. Myenteric plexuses were dissected from the ileum of WT and HB-EGF KO mice. (**a**,**c**) Whole-mount IHC using antibodies to the neuronal marker HuC/D, and the functional neuronal cell markers nNOS and ChAT. Scale bar = 10 µm. (**b**,**d**) Fold changes in nNOS and ChAT immunofluorescence staining density in HB-EGF KO myenteric ganglion cells relative to WT. $^*P < 0.05$, $n = 3$ animals in each group. (**e**,**f**) Tissue proteins were extracted from the intramuscular layers of WT and KO small intestine and subjected to western blotting using anti-nNOS and anti-ChAT antibodies, with densitometry confirming significantly decreased nNOS and increased ChAT expression in ganglia from HB-EGF KO mice. $^*P < 0.05$ compared with WT. $n = 3$ independent experiments. (**g**,**h**) Primary enteric neuron cell cultures from HB-EGF KO and WT mice. E12.5 mouse embryonic gut was harvested and digested with collagenase and dispase. Dissociated cells were plated in eight-well plates coated with poly-D-lysine and laminin. Neuronal cells and their neurites were stained with the pan-neuronal cell marker PGP 9.5 after 3 days in culture. Using Image-Pro software, neurites were traced and the length of the longest neurite extension from the cell body was measured. The percentage of cells bearing neurites was also estimated. At least 100 cells isolated from three different WT and KO mice were scored. $^*P < 0.05$ (Student's *t*-test). Mean ± s.e.m. Scale bar = 25 µm. ChAT, choline acetyl transferase; HB-EGF, heparin-binding EGF-like growth factor; IHC, immunohistochemistry; KO, knockout; nNOS, neuronal nitric oxide synthase; WT, wild type.

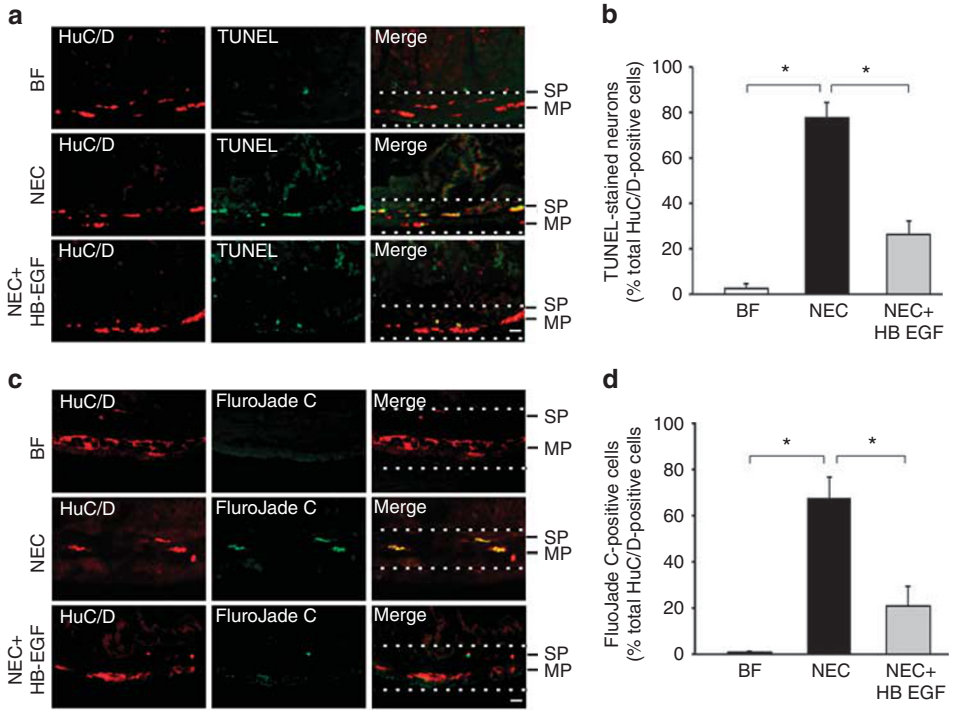

Figure 6. HB-EGF reduces NEC-induced neuronal apoptosis and degeneration. Ileum was harvested from pups that were BF, exposed to NEC, or exposed to NEC but treated with HB-EGF added to each feed. (**a**) Tissue sections were double-stained with the neuronal marker HuC/D (red) and TUNEL (green) to demonstrate apoptosis localized to the SP and MP. (**b**) Quantification of the percentage of TUNEL-stained neurons in the ENS layer (between the two white dashed lines) consisting of SP and MP. (**c**) Tissue sections were double-stained with the neuronal marker HuC/D (red) and FluroJadC (green). (**d**) Quantification of the percentage of double-positive stained cells in the ENS layer. Intestinal neuronal apoptosis and degeneration in the ENS was significantly increased in pups exposed to NEC and decreased in pups exposed to NEC but treated with HB-EGF. Quantification of these cells was based on 10 serial intestinal cross-sections of each individual animal from the BF, NEC, and NEC+HB-EGF groups ($n = 4$–9 pups). *$P < 0.05$ (Dunnett's *post hoc* analysis). Scale bar = 25 µm. BF, breast fed; ENS, enteric nervous system; HB-EGF, heparin-binding EGF-like growth factor; MP, myenteric plexus; NEC, neonatal necrotizing enterocolitis; SP, submucosal plexus; TUNEL, terminal deoxynucleotidyl transferase nick-end labeling.

nitrergic neural activity shaping late-differentiating neurons in the developing ENS (17). We demonstrate here that HB-EGF enhances robust expression of nNOS during early NSC differentiation *in vitro*, suggesting that the ability of HB-EGF to promote NSC differentiation may be regulated by increased numbers of nNOS neurons and subsequently enhanced NO production. In addition, we found that HB-EGF promotes nNOS expression only in newly differentiated neurons or glial cells, and not in undifferentiated NSCs (Zhou's unpublished data). A dose of a general NOS inhibitor suppresses the ability of HB-EGF to promote neural differentiation, and triggers a switch from differentiation to proliferation of NSCs. Furthermore, selective inhibition of the nNOS isoform blocks HB-EGF-induced neural differentiation, suggesting that nNOS-derived NO exerts a specific effect in the differentiation of NSC. A single dose of a specific nNOS inhibitor applied to early-differentiating neurospheres blocks HB-EGF-induced NSC differentiation, suggesting that the presence of nNOS-expressing cells during the early differentiation of NSCs is essential for the subsequent neural differentiation cascade. A similar report using an *in vivo* model showed that the lack of anchoring nNOS-positive cells during embryonic stages led to failed enteric NSC migration, colonization, and maturation in the gut (17). Collectively, these results suggest that paracrine NO signaling of nNOS-expressing cells is an essential mediator of HB-EGF-induced neural differentiation.

Using HB-EGF KO mice, we identified a pronounced decrease in nNOS-expressing neurons with an increase in ChAT-expressing neurons in the MP. HB-EGF is an important mediator for generating or maintaining a normal subpopulation of nitrergic and cholinergic neurons in the ENS. During the developmental stage of the ENS in HB-EGF KO mice, deficiency of nNOS-derived NO production may contribute to compromised neuronal maturation given the decrease in neurite-extending cells and the short neurite extensions from enteric neurons isolated from these mice. In addition, deficiency of nNOS or HB-EGF expression is associated with a lack of ability to remodel or restore the ENS during physiological changes or after intestinal damage. For example, compromised intestinal motility associated with a selective decrease in the numbers of nNOS-expressing neurons in the intestine was observed in aged animals (18). Myenteric neuronal degeneration and intestinal motility

disorders have been documented in HB-EGF KO and nNOS KO mice (9,19). Similar reports have shown that HB-EGF KO or nNOS KO mice have increased susceptibility to experimental NEC or intestinal ischemia/reperfusion injury (7,20). Clearly, nNOS-derived NO protects the ENS from neuronal degeneration or damage.

Recently, we documented that human neonatal NEC is associated with ENS alternations, particularly loss of nNOS-expressing neurons (4). In the present study, we demonstrate the protective effects of HB-EGF on the ENS after experimental NEC, with improved nNOS expression and decreased neuronal apoptosis and degeneration. As intestinal motility is mainly regulated by myenteric neurons, the preserved ENS integrity noted after HB-EGF treatment is likely responsible for the improved intestinal motility during experimental NEC that we have previously reported (10). It is noteworthy that the preservation of nNOS expression in the intestine protected the ENS from injury. There exist several potential mechanisms by which nNOS-derived NO could protect the ENS. First, nNOS-derived NO may directly mediate neuroprotection by reducing apoptotic neuronal cell death, as this "housekeeping" neuroprotective effect was severely compromised in nNOS KO mice after peripheral nerve transection (21). Preservation of nNOS expression in the nervous systems is of significance, as it is associated with suppression of excessive iNOS activity (22), which is correlated with neuronal damage. In addition, NO production regulates numerous essential functions of the gastrointestinal tract, such as maintenance of adequate intestinal microvascular perfusion, proper intestinal motility, regulation of epithelial permeability, and regulation of the immune response (23). The constitutive production of NO exerts anti-inflammatory effects via modulation of platelet homotypic aggregation and platelet adhesion (24). NO also alters the cytokine profile released by macrophages, and inhibits intestinal bacterial translocation during intestinal ischemia or inflammation injury (25,26).

Importantly, this is the first report showing that HB-EGF preserves glial cells during NEC *in vivo*, and increases nNOS expression in glial cells *in vitro*. Previous evidence has shown that ablation of enteric glial cells leads to fulminant inflammation in the intestine, similar to NEC, and is characterized by increased myeloperoxidase activity, intraluminal hemorrhage and degeneration of myenteric neurons, and acute loss of enteric glial cells (27). Lack of reactive enteric glial cells is somewhat surprising, given that ischemia and inflammation are powerful stimuli for astrocyte reaction in the central nervous system (28). In the ENS, intrinsic immaturity or failure of enteric glial cells to respond to ischemic or inflammatory insults may precipitate the injury that results in NEC in premature neonates. As recent evidence strongly suggests that ablation of enteric glial cells may be an upstream target of NEC pathology (29), the ability of HB-EGF to preserve GFAP-expressing reactive glial cells is critical, as HB-EGF may promote glial cell maturation or exert protective effects directly. In addition, it is also possible that HB-EGF drives glial cell de-differentiation and promotes glial cell-derived neurogenesis to replenish neuronal loss after NEC injury. Although the roles of increased nNOS expression in glial cells remain unclear, nNOS produced by glial cells suppresses nuclear factor Kappa B activation and subsequently reduces iNOS expression (22). We have previously reported that HB-EGF suppresses iNOS expression and cytotoxic peroxynitrite production in the intestine during experimental NEC (30). Our current results show that HB-EGF-induced nNOS production in intestinal glial cells may also contribute to the suppressive effects of HB-EGF on iNOS expression and peroxynitrite production in the injured intestine.

In summary, we demonstrate that HB-EGF promotes the differentiation of enteric NSCs into neurons in an NO-dependent manner. We also provide strong evidence that neurons and glial cells are injured during NEC, and that administration of HB-EGF preserves nNOS expression and protects the ENS from NEC-induced injury. These findings may enable us to best exploit the potential of HB-EGF therapy in restoring ENS integrity and intestinal motility after clinical NEC in the future.

AUTHOR CONTRIBUTIONS

Y.Z. conceived the study, carried out all experiments, acquired and interpreted the data, and wrote the manuscript. Y.W. performed flow cytometry and interpreted the data. J.O. and J.Y. developed the experimental NEC model. G.E.B. carried out critical revision of the manuscript, and obtained funding for all of the studies presented. All authors read and approved the final manuscript.

STATEMENT OF FINANCIAL SUPPORT

This work was supported by the National Institutes of Health R01 GM61193 and R01 GM113236.

Disclosure: The authors declare no conflict of interest.

REFERENCES

1. Berseth CL. Gestational evolution of small intestine motility in preterm and term infants. J Pediatr 1989;115:646–51.
2. Winston JH, Li Q, Sarna SK. Paradoxical regulation of ChAT and nNOS expression in animal models of Crohn's colitis and ulcerative colitis. Am J Physiol Gastrointest Liver Physiol 2013;305:G295–302.
3. Zaitoun I, Erickson CS, Barlow AJ, et al. Altered neuronal density and neurotransmitter expression in the ganglionated region of Ednrb null mice: implications for Hirschsprung's disease. Neurogastroenterol Motil 2013;25:e233–44.
4. Zhou Y, Yang J, Watkins DJ, et al. Enteric nervous system abnormalities are present in human necrotizing enterocolitis: potential neurotransplantation therapy. Stem Cell Res Ther 2013;4:157.
5. Besner G, Higashiyama S, Klagsbrun M. Isolation and characterization of a macrophage-derived heparin-binding growth factor. Cell Regul 1990;1:811–9.
6. Radulescu A, Zhang HY, Yu X, et al. Heparin-binding epidermal growth factor-like growth factor overexpression in transgenic mice increases resistance to necrotizing enterocolitis. J Pediatr Surg 2010;45:1933–9.
7. Radulescu A, Yu X, Orvets ND, et al. Deletion of the heparin-binding epidermal growth factor-like growth factor gene increases susceptibility to necrotizing enterocolitis. J Pediatr Surg 2010;45:729–34.
8. Nakagawa T, Sasahara M, Hayase Y, et al. Neuronal and glial expression of heparin-binding EGF-like growth factor in central nervous system of

prenatal and early-postnatal rat. Brain Res Dev Brain Res 1998;108:263–72.
9. Zhou Y, James I, Besner GE. Heparin-binding epidermal growth factor-like growth factor promotes murine enteric nervous system development and enteric neural crest cell migration. J Pediatr Surg 2012;47:1865–73.
10. Wei J, Zhou Y, Besner GE. Heparin-binding EGF-like growth factor and enteric neural stem cell transplantation in the prevention of experimental necrotizing enterocolitis in mice. Pediatr Res 2015;78:29–37.
11. Michalsky MP, Lara-Marquez M, Chun L, et al. Heparin-binding EGF-like growth factor is present in human amniotic fluid and breast milk. J Pediatr Surg 2002;37:1–6.
12. Chen CL, Yu X, James IO, et al. Heparin-binding EGF-like growth factor protects intestinal stem cells from injury in a rat model of necrotizing enterocolitis. Lab Invest 2012;92:331–44.
13. Lefebvre RA. Nitric oxide in the peripheral nervous system. Ann Med 1995;27:379–88.
14. Hoshino H, Uchida T, Otsuki T, et al. Cornichon-like protein facilitates secretion of HB-EGF and regulates proper development of cranial nerves. Mol Biol Cell 2007;18:1143–52.
15. Estephane D, Anctil M. Retinoic acid and nitric oxide promote cell proliferation and differentially induce neuronal differentiation *in vitro* in the cnidarian Renilla koellikeri. Dev Neurobiol 2010;70:842–52.
16. Branchek TA, Gershon MD. Time course of expression of neuropeptide Y, calcitonin gene-related peptide, and NADPH diaphorase activity in neurons of the developing murine bowel and the appearance of 5-hydroxytryptamine in mucosal enterochromaffin cells. J Comp Neurol 1989;285:262–73.
17. Hao MM, Moore RE, Roberts RR, et al. The role of neural activity in the migration and differentiation of enteric neuron precursors. Neurogastroenterol Motil 2010;22:e127–37.
18. Johnson RJ, Schemann M, Santer RM, et al. The effects of age on the overall population and on sub-populations of myenteric neurons in the rat small intestine. J Anat 1998;192(Pt 4):479–88.
19. Rivera LR, Poole DP, Thacker M, et al. The involvement of nitric oxide synthase neurons in enteric neuropathies. Neurogastroenterol Motil 2011;23:980–8.
20. Rivera LR, Pontell L, Cho HJ, et al. Knock out of neuronal nitric oxide synthase exacerbates intestinal ischemia/reperfusion injury in mice. Cell Tissue Res 2012;349:565–76.
21. Keilhoff G, Fansa H, Wolf G. Neuronal NOS deficiency promotes apoptotic cell death of spinal cord neurons after peripheral nerve transection. Nitric Oxide 2004;10:101–11.
22. Qu XW, Wang H, De Plaen IG, et al. Neuronal nitric oxide synthase (NOS) regulates the expression of inducible NOS in rat small intestine via modulation of nuclear factor kappa B. FASEB J 2001;15:439–46.
23. Lanas A. Role of nitric oxide in the gastrointestinal tract. Arthritis Res Ther 2008;10(Suppl 2):S4.
24. Radomski MW, Palmer RM, Moncada S. Endogenous nitric oxide inhibits human platelet adhesion to vascular endothelium. Lancet 1987;2:1057–8.
25. Huang FP, Niedbala W, Wei XQ, et al. Nitric oxide regulates Th1 cell development through the inhibition of IL-12 synthesis by macrophages. Eur J Immunol 1998;28:4062–70.
26. Nadler EP, Ford HR. Regulation of bacterial translocation by nitric oxide. Pediatr Surg Int 2000;16:165–8.
27. Bush TG, Savidge TC, Freeman TC, et al. Fulminant jejuno-ileitis following ablation of enteric glia in adult transgenic mice. Cell 1998;93:189–201.
28. Streit WJ. Microglial response to brain injury: a brief synopsis. Toxicol Pathol 2000;28:28–30.
29. Bush TG. Enteric glial cells. An upstream target for induction of necrotizing enterocolitis and Crohn's disease? Bioessays 2002;24:130–40.
30. Lara-Marquez ML, Mehta V, Michalsky MP, et al. Heparin-binding EGF-like growth factor down regulates proinflammatory cytokine-induced nitric oxide and inducible nitric oxide synthase production in intestinal epithelial cells. Nitric Oxide 2002;6:142–52.